SARS-CoV-2 Vaccine Effectiveness for Patients Undergoing Immunosuppressive Treatment

By Grayson Coleman

Department of Nephrology and Hypertension, UNC Kidney Center, UNC School of Medicine

Senior Honors Thesis University of North Carolina at Chapel Hill Department of Biology

6 December 2023

Approved:

_____

Dr. Ronald Falk, Research Mentor

Dr. Meghan Free, Thesis Advisor

Dr. Ben Philpot, Reader

Dr. Alaina Garland, Reader

Abstract

The urgency spurred by the SARS-CoV-2 pandemic has propelled an essential shift towards investigating the efficacy of vaccinations in protecting immunosuppressed patients. We honed our investigations on the efficacy of the SARS-CoV-2 vaccine suspecting these patients would have lower protection against the virus than healthy controls due to a reduced and/or inhibited adaptive immune repertoire. Peripheral T cells were analyzed to determine proliferation fitness as well as measure the activation of Th1, Th17, and Tfh subtypes through cytokine analysis. Patients demonstrated varying degrees of protection against the novel coronavirus compared to healthy controls. Further inspection also demonstrated an influx of IFNy production in both healthy controls and patients following booster vaccination (the third vaccine received). Cytokine analysis showed no significant differences in cytokine production in these subtypes between healthy controls and immunosuppressed patients which would correlate to a difference in immune capability. These findings demonstrated that patients and healthy controls produced similar responses to the RBD peptide leading us to believe patient T cells may not be greatly impacted by immunosuppressive therapies. Percent inhibition of neutralizing antibodies to the SARS-CoV-2 antigen were then subsequently calculated from peripheral B cells to determine their immune fitness. The resulting data demonstrated that immunosuppressed patient B cells elicited either an *inadequate*, *moderate*, or *adequate* antibody response. The three clusters identified, we believe, are governed by an unidentified indicator not directly related to primary demographic information, though, tethered to the timing of patient immunosuppressive treatment administration. These results underscore the

importance of addressing vaccination strategies for immunosuppressed patients, highlighting the need for tailored approaches to ensure their protection and greater public safety.

Introduction

Background

The 2020 Pandemic was a wake-up call for many, particularly in the realm of public health. It was an unprecedented event with an impact that is palpable still some three years later. The SARS-CoV-2, now endemic, proves an opportune time to investigate many questions regarding vaccine immunology often pondered by scientists but left understudied due to their lack of priority[1]. Priority has now shifted in favor of answering these questions, chief of which for the UNC Kidney Center being how immunosuppressed individuals respond to vaccinations and the level of protection being marketed to them. With the reported intended plan by the Center for Disease Control (CDC) to issue seasonal SARS-CoV-2 vaccinations, it is time this matter was elucidated[2].

Immunosuppressed adult persons in the United States accounted for 12.2% of COVID-19 hospitalizations between the years of 2020 and 2022 while only making up an estimated 3% of the total population[3]. The immunosuppressed, immunocompromised, and immunodeficient population have long been labeled as “at risk” for various virulent pathogens, however, little has been done on behalf of the medical community to provide proper defense[4,5,6]. Much of the responsibility is placed on the shoulders of these patients when it should be on the men and women behind the bench. We have taken that initiative and are pleased with the directions in which our data positions this topic.

Current Literature on the Immunosuppressed and SARS-CoV-2

Graphic 1: A Brief History of the SARS-CoV-2 Virus

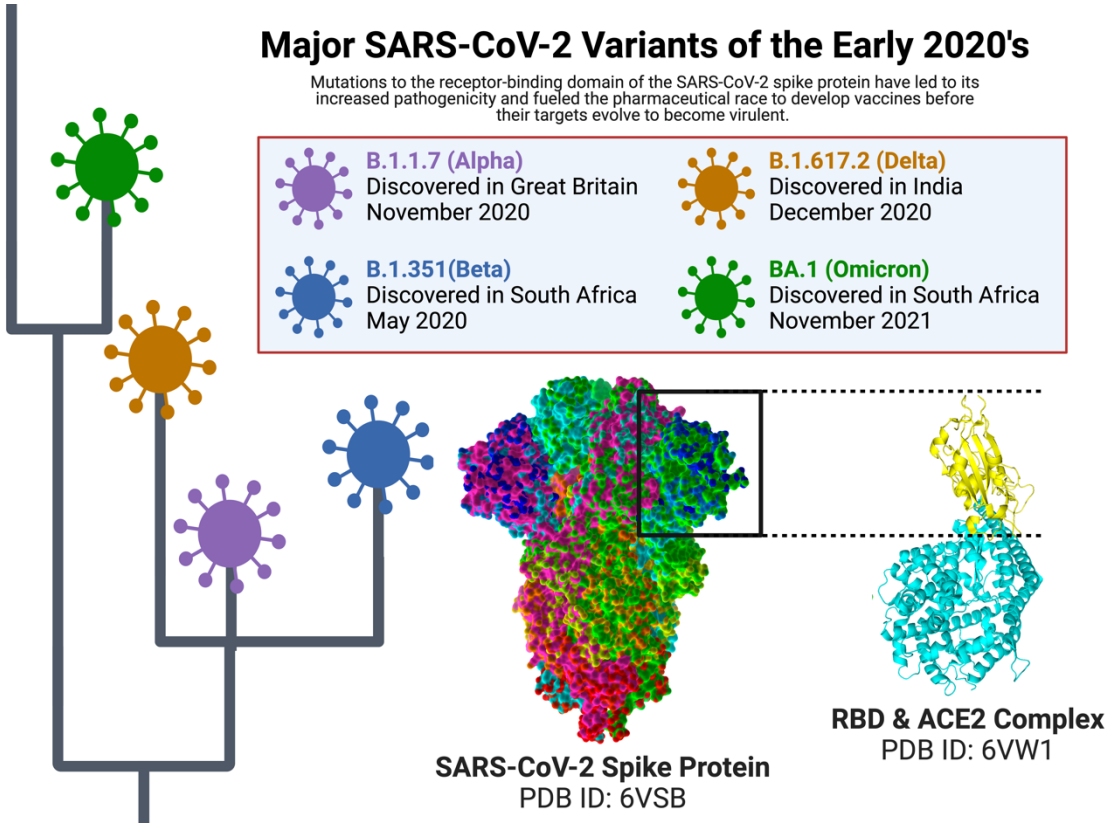

Phylogeny of the SARS-CoV-2 virus and its prominent variants from 2020 to 2023 and onward (**left**) complimented with color coded legend including scientific name of variant, colloquial name of variant, location of discovery and date of discovery (**top**)[7,8,9]. Three-dimensional rendering of the virus' spike protein (**bottom center**) with an inspected view of the tertiary structure of the protein's RBD region and ACE2 complex of which the virus binds to upon infection (**bottom right**)[10,11].

Singson et al. and the CDC COVID-NET Surveillance Team demonstrated in a metareview that low correlation existed between immunocompromised individual vaccination status and ICU admission or in-hospital death[3]. In the same study, the authors showed that there was a correlation between non-immunocompromised individual vaccination status and ICU admission and in-hospital death (aOR = 1.01 and 1.34 respectively with CI of 95%). This identifies a major hole in the current logic being projected in public health discussions. Though vaccination status in immunocompetent individuals seems to provide an indicator for disease severity, the

correlation with the immunocompromised seem to be inconsequential. Does this mean the SARS-CoV-2 vaccine is a waste of resources for the immunocompromised? Certainly not – though vaccination may not affect disease severity for the immunocompromised, there is another aspect of immunity in which the vaccine may be playing a preventative role. Bahremand et al. showed in a recent publication the hospitalization rates for various immunocompromised groups with COVID-19 stratified by vaccination status[12]. Among the most immunocompromised individuals (CEV 1 / Clinically Extremely Vulnerable 1), the authors showed nearly a 50% decrease in hospitalization rates between individuals who received their second vaccine (initial vaccination 2 out of 2) and their third vaccine (booster vaccination). In addition, they showed the progression of hospitalization rates longitudinally in which with each additional vaccine each CEV group received, their rate of hospitalization decreased on average by 10% per dose. This shows that though vaccines do not appear to correlate with immunosuppressed patient COVID-19 infection severity, the vaccines do correlate with a severely decreased instance of disease onset.

Where The Literature Ends and Where We Began

Having appreciated the novelty not only of the environment we were living under but also of our research query, we established a study structure with the intent of assuming as little as necessary. Additionally, we set out knowing that vaccination status influenced protection rather than disease severity which greatly emphasizes the importance of elucidating whether immunosuppressed patients were receiving proper protection. Branched into a T cell arm and B cell arm, we analyzed immunosuppressed lymphocytes both qualitatively by asking whether the

cell types would activate when exposed to the SARS-CoV-2 antigen and quantitatively by asking whether the cell types could properly defend themselves when exposed to the SARS-CoV-2 antigen.

We identified patient demographics of high interest based upon their immunosuppressive therapy from their treatment plan and their chronic disease.

Graphic 2: SARS-CoV-2 Infection in the Human Periphery

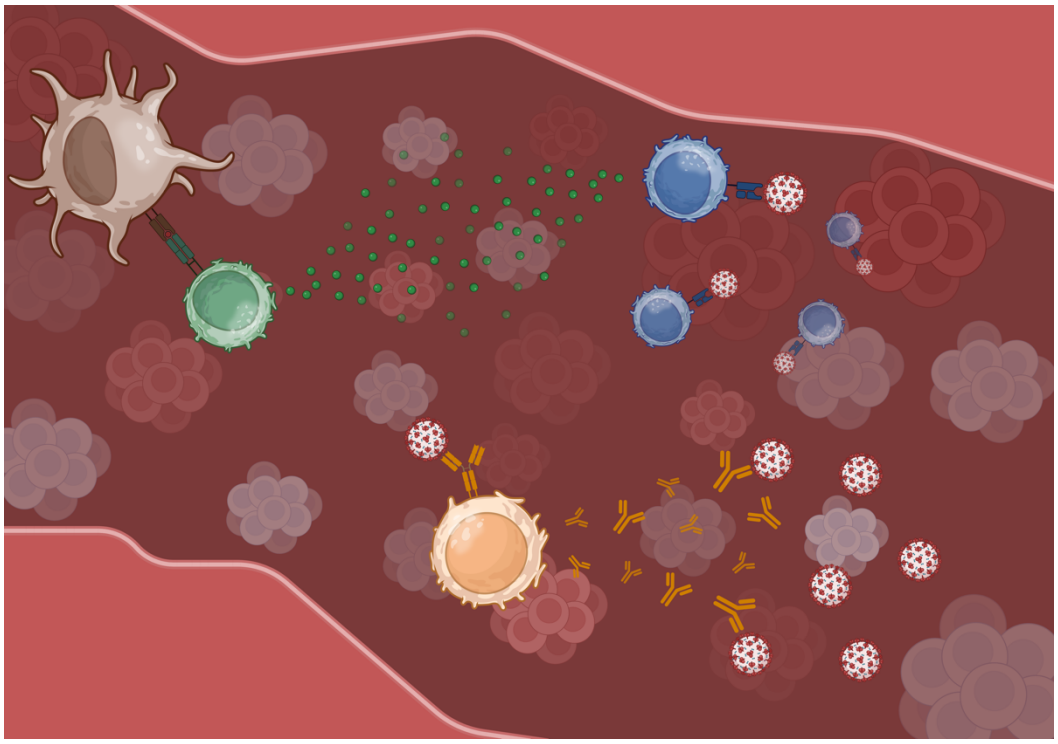

The human immune response progressing from left to right starting with the presentation of the SARS-CoV-2 by the dendritic cell (**brown**) to the CD4+ T cell's (**green**) MHC-2 receptor. A vast array of cytokines are then released signaling the activation of CD8+ T cells (**blue**) to begin attack against the pathogen. Concurrently, human B cells (**orange**) are encountering the virus's spike protein with their BCR and are thereby activated to begin producing neutralizing antibodies[13,14].

Patient therapies included rituximab, mycophenolate mofetil (MMF), azathioprine, methotrexate, Plaquenil, and prednisone. Rituximab is an ad-hoc CD20 monoclonal antibody IV infusion which is commonly used in the treatment of cancer cells which highly express this marker and B cells (the target of interest for our research)[15]. MMF is traditionally used as a transplant medication and is typically supplemented with other medications to repress immune

activation[16]. Its targets include both T cells and B cells through inhibiting lymphocyte cellular activity (the exact target is inosine-5'-monophosphate which is key in purine synthesis). Azathioprine, similarly, is conventionally used in organ transplant patients[17]. It preferentially targets T cells through disrupting their DNA and RNA synthesis. Methotrexate is a disease-modifying anti-rheumatic drug (DMARD) and is prescribed as an anti-metabolite that predominantly targets T cell activity[18]. Hydroxychloroquine (generic name for the name brand medication Plaquenil) is an anti-inflammatory and also a DMARD[19]. It's mechanisms of action are relatively unknown, though, it has been identified as a successful treatment of rheumatoid arthritis and systemic lupus in erythematosus. Prednisone is a potent corticosteroid which works by binding to human glucocorticoid receptors resulting in handicapped immune cells and inflammatory mediators[20].

We investigated and grouped patients by their disease involvement which included vasculitic, rheumatologic, nephrologic, more than one, and other conditions not specified. *Vasculitic* condition involvement included granulomatosis with polyangiitis (GPA), microscopic polyangiitis (MPA), and eosinophilic granulomatosis with polyangiitis (EGPA) which primarily impact patient vascular systems[21,22,23]. *Rheumatologic* condition involvement included Systemic Lupus Erythematosus (SLE), Rheumatoid Arthritis (RA), and Sjogren's Syndrome which impede patients globally[24,25,26]. *Nephrologic* condition involvement included Lupus Nephritis, IgA nephropathy, membranous nephropathy, focal segmental glomerulosclerosis (FSGS), and minimal change disease which all impact patient kidneys[27,28,29,30,31]. Some patients did not fit into any of these three categories due to being members of more than one or by having unique conditions that fit them into none.

We were acutely aware that our focus extended beyond the binary notion of vaccination status as a mere determinant of infection[32]. Instead, we understood that it was the influence of vaccination on protection rather than disease severity that bore paramount significance. This premise underscored the critical importance of our pursuit: to shed light on whether immunosuppressed patients were, in fact, receiving the full measure of protection they deserved.

Methods

3.1 Sample Acquisition, PBMC Cryopreservation, and PBMC Thawing

A cohort of 101 study participants (patient n=89, healthy control n=12) were consented and provided blood samples over the course of 25 months between the months of July 2020 and September 2022. All participants were enrolled through UNC Health affiliated clinics including the Department of Nephrology, Department of Rheumatology, and Department of Dermatology. Participant selection centered on the following:

Patient Inclusion Criteria

1. *Age ≥ 2 years old*
2. *Patient with vasculitis, glomerular diseases, or other autoimmune diseases*
3. *Able to provide informed consent and assent when age appropriate*
4. *Willingness to comply with study requirements, including an intention to participate in study follow-up and biospecimen collection*

5. *Plan to receive vaccination 1-3 months following enrollment or have completed SARS-CoV-2 vaccination course within the prior 1-3 months*

Patient Exclusion Criteria

1. *Age less than < 2 years old*
2. *History of splenectomy*
3. *History of cancer with exposure to chemotherapy in the last two years*
4. *Any active COVID-19 infection at the time of enrollment*
5. *Has participated in another investigational study and received an immunomodulatory investigational drug in the last 12 months before enrollment (the timeline is subject to change per PI discretion depending on the half-life of the investigational drug)*
6. *History of uncontrolled HBV, HCV, and/or HIV*
7. *Has received blood, blood products, or IVIG in the last three months*
8. *Unable or unwilling to give a comprehensive informed consent*
9. *Unable or unwilling to comply with study procedures and visit schedule*
10. *Institutionalized individuals*
11. *Patients on renal replacement therapy*
12. *Solid organ or bone marrow transplant recipient*

Healthy Control Exclusion Criteria

1. *PMH of COPD, Diabetes, liver cirrhosis, cancer, chronic infection, asthma, severe allergic reaction to vaccine*

2. *On any of the following: immunosuppressive medications, IVIG*

3. *Recent blood transfusion*

Graphic 3: Broad View of Sample Acquisition Timeline

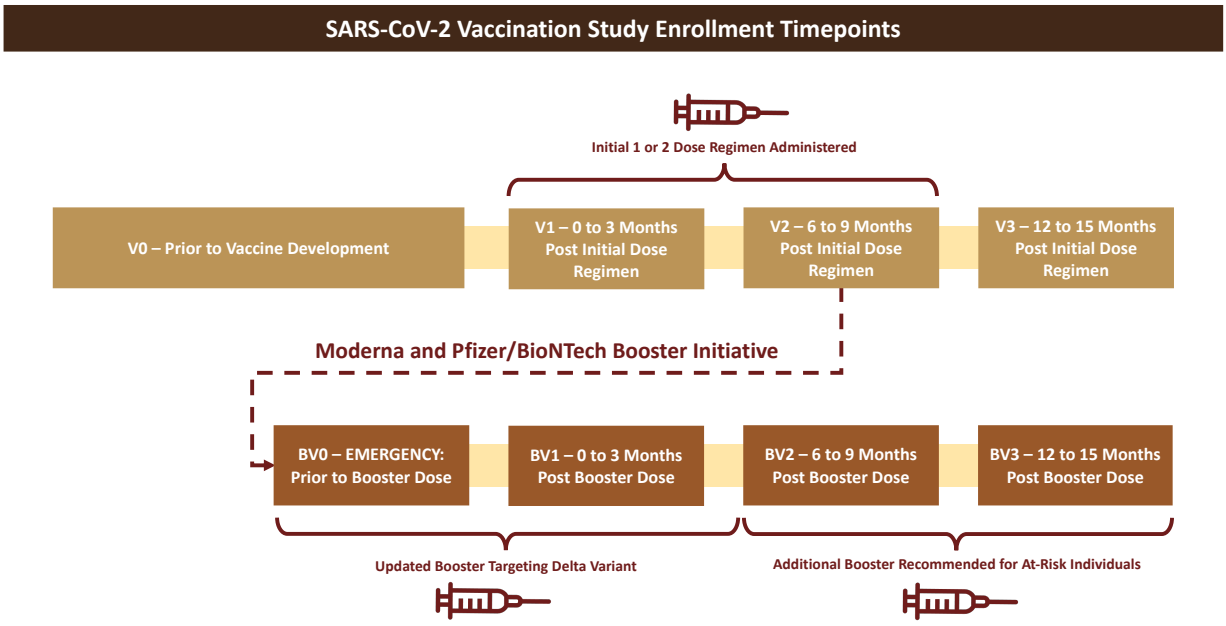

Total of eight timepoints displayed with V0, V1, V2, and V3 representing sample collections centered on the initial doses of the SARS-CoV-2 vaccine and BV0, BV1, BV2, and BV3 representing sample collections centered on the booster vaccine targeting the Delta variant of the virus. Samples were collected in 0 to 3 month, 6 to 9 month, and 12 to 15 month increments. Syringe graphic is used to symbolize when a new vaccine was issued and probably administered to subjects. Samples were collected over the course of approximately two years.

Eight timepoints were available for sample collection (Graphic 3), though, timepoints V0, V1, V2, BV1, BV2, BV3 were the six most successful in obtaining samples. The original study timeline was structured to obtain samples at 5-month intervals, with a 3-month collection period per timepoint. However, an unforeseen development occurred between the study's V2 and V3 timepoints when Pfizer/BioNTech and Moderna introduced their booster initiatives. This necessitated an emergency deviation from the original study plan, diverting our focus from continuing with V3 data acquisition to collecting BV0 samples immediately before booster administration. As a result of this abrupt change, BV0 and V3 timepoints acquired the fewest

samples in our dataset. Choice to vaccinate and choice of vaccination formula was voluntary and up to the subject's discretion.

Table 1: Total Patient Demographics

Diagnosis		Sample Visit		Vaccine Formula		Therapy		Race & Ethnicity	
Lupus Nephritis	3	V0	46	Pfizer/ BioNTech	48	Prednisone	4	White	65
Systemic Lupus Erythematous	2	V1	79	Moderna	40	Solumedrol	1	Black	11
Rheumatoid Arthritis	1	V2	30	Johnson & Johnson	1	Rituximab	39	Asian	5
Sjogren's Syndrome	0	V3	3			Cyclophosphamide	3	Hispanic/Latino	5
GPA	27	BV0	7			MMF	20	Native American/ Pacific Islander	1
MPA	12	BV1	37			Tacrolimus	1	More Than One	2
IgA Nephropathy	3	BV2	34			Plaquenil	2		
Membranous Nephropathy	2	BV3	55			Azathioprine	7		
FSGS	1					Methotrexate	3		
Minimal Change Disease	2					Other	9		
Other	26								
More Than One	10								

Demographic data on cumulative patients enrolled (n=89) with a mean age of 56 years old (SD of 22 years). Patient diagnosis, vaccine formula, therapy, race and ethnicity, age, among other variables were recorded. Data is displayed left to right as the number from the total sample size per diagnosis, per visit collected, per vaccine formula, per therapy, and per race/ethnicity. Patients with "More Than One" diagnosis were exclusively placed in this category while all other categories were reserved for patients with only one diagnosis (meaning a patient with Lupus Nephritis and MPA would be placed in "More Than One" rather than in "Lupus Nephritis" and/or in "MPA). Patient therapy was categorized by primary therapy. Backtracking is underway to elicit full medication regimen per patient. These same methods are also concurrently being conducted on healthy controls.

All samples were isolated for their peripheral blood mononuclear cells (PBMCs) and cryopreserved in liquid nitrogen. PBMCs were stored at 1 mL using dimethyl sulfoxide (DMSO) at a cell concentration of 5E6/mL. Frozen PBMCs were thawed and washed at the start of each assay with a cell media containing RPMI 1640 supplemented with 10% fetal bovine serum and HEPES buffer solution. PBMCs were thawed using this cell media and incubated at 37°C in a CO_2

environment for one hour. Cells were then counted and aliquoted to the assay-specific concentration.

3.2 T cells

3.2.1 ELISpot Assay

One monoclonal antibody and two peptide pools were used in the ELISpot analyses. MabTech's anti-human mAb CD3-2 (MabTech, 3605-1S) was used as a positive control and provided a reliable stimulus to measure absolute T cell IFNy production. The CEFX PepMix (JPT, PM-CEFX-2) was used as an immune fitness metric for practical T cell IFNy production. The newest integration from the earlier CEF peptide pool contained several short amino acid chains (9-15 amino acids) covering 176 epitopes from multiple commonly immunized antigens. An RBD PepMix (JPT, PM-WCPV-S-RBD-1) was used as an experimental stimulus. The RBD pool contained 53 peptides derived from the RBD of the SARS-CoV-2 spike glycoprotein, which was the target of most COVID-19 vaccines. These stimulants were diluted to a concentration of 1:1000, 1:200, 1:200 respectively.

These three master mixes were used to stimulate the PBMCs, with a fourth well serving as a negative control (mock well containing cell media with no stimulants). Each sample was tested under these four conditions, with duplicates for each, making a total of eight wells per sample.

All ELISpot assays were run using MabTech ELISpot Pro for Human IFNy assay (MabTech, 3420-2HPT-10).

Figure 1: ELISpot Plate Model

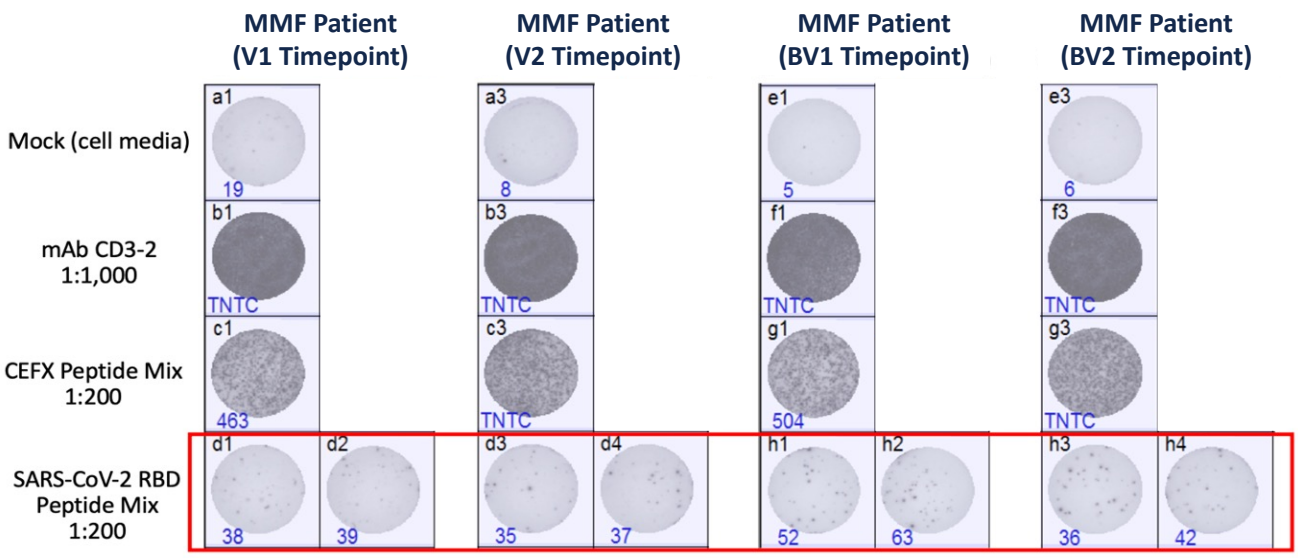

This model was taken from a patient at V1, V2, BV1, and BV2. ELISpots were performed on a 96-well plate with columns 1 through 12 and rows A through H. The model was formatted on a four by eight grid reading from left to right V1 to V2 in the upper row (rows A, B, C, and D) to BV1 to BV2 in the lower row (rows E, F, G, and H). Duplicates were run for each condition. Only RBD duplicates are visible on this model. Each "spot" represents where one single cell implanted itself and secreted IFNy in response to its given condition. Counts were positioned in the lower left corner of each well in blue with values ranging from zero (no secretion) to TNTC (abbreviated for "too numerous to count"). TNTC was estimated to be activated by the software around 600 spots or more. The first row (rows A and E) was treated using cell media with no stimulation. The second row (rows B and F) was treated with anti-human CD3. The third row (rows C and G) was treated with CEFX PepMix. The fourth and final row (rows D and H) was treated with the SARS-CoV-2 RBD peptide.

Prior to plating, the ELISpot plate was washed with PBS and blocked with cell media. Samples at a cell concentration of 3.5E5/100µL in cell media were then added in a descending vertical order to the plate as follows: a negative control mock well containing 100µL of cell media, a positive control well containing 100µL of the mAB CD3-2 master mix, an immune fitness well containing 80µL of the CEFX PepMix, and an experimental well containing 80µL of the RBD PepMix. After adding these conditions to their respective wells, 100µL of the

suspended cells were added from their respective aliquots. These plates were then sealed in parafilm and incubated for eighteen hours at 37°C in a CO_2 environment to allow IFNy release.

Following this incubation, the plate had a series of PBS washes followed by 100µL of detection antibody master mix (7-B6-ALP diluted 1:200). Plates then rested at room temperature for two hours. Once complete, the plate was washed with PBS and received 100µL of substrate per well to be developed over the next ten minutes. The plate was then extensively washed under distilled water to halt the reaction. Finally, the plate was stored away from light to dry before being imaged.

3.3.1 Flow Cytometry Studies

Graphic 4: T cell Subsets of Interest, Their Cytokine Milieus, and Their Functions

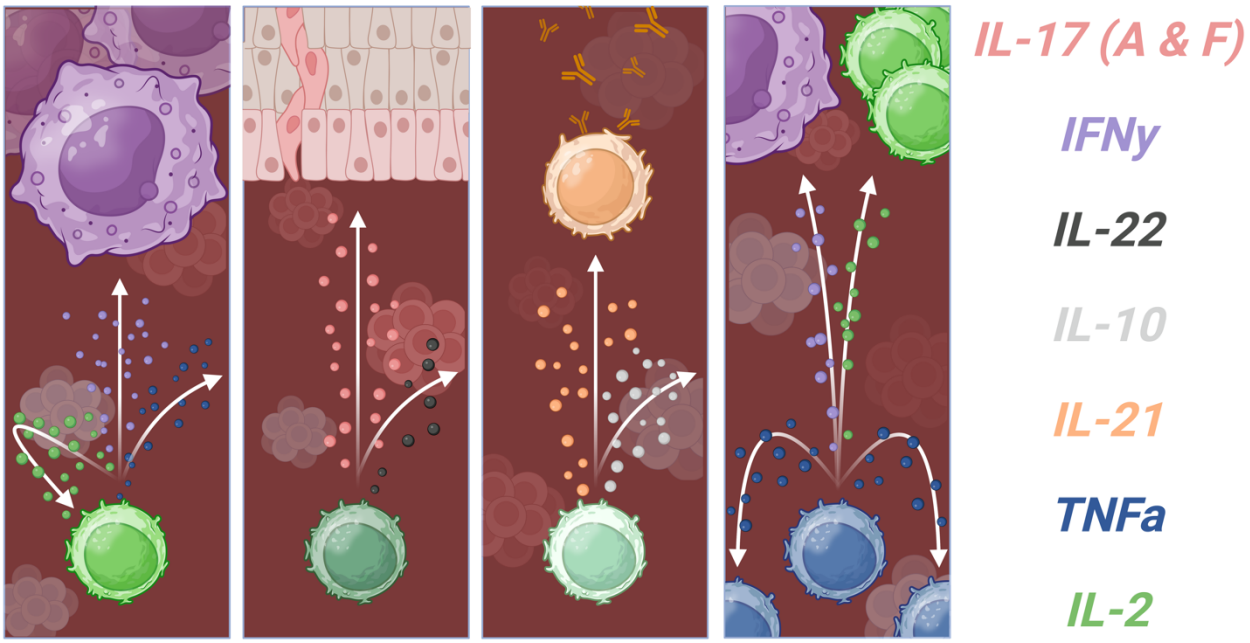

Far Left Neon T Helper cell 1 (Th1) releasing INFy to activate macrophages (**purple**), TNFa to activate cytotoxic T cell repertoire, and IL-2 to increase proliferation and activation[33]. **Left Center Dark Green** T Helper cell 17 (Th17) releasing IL-17A and IL-17F to activate epithelial cells for recruitment and other inflammatory signaling as well as IL-22 which generates localized defensins[34]. **Right Center Pale Green** T follicular helper cell (Tfh) releasing IL-21 to alert/activate B cell antibody activity and IL-10 to regulate the T cell immune response and prevent over stimulation[35]. **Far Right Blue** Cytotoxic T cell (CD8) releasing the same milieu as Th1 cells to support the T cell response[36,37].

Our flow cytometry panel contained ten anti-human antibodies corresponding to the eight cytokines of interest along with CD4 and CD8 to identify helper and cytotoxic T cells. Each antibody was selected to identify specific T cell subsets to determine population differences over time between healthy controls and diseased patients. T cell subsets of interest included Th1 (identified by $CD4^+$ secreted IFNy, IL-2, and TNFa), Th17 (identified by $CD4^+$ secreted IL-22, IL-17F, and IL-17A), and Tfh (identified by $CD4^+$ secreted IL-21 and IL-10). $CD8^+$ secreted IFNy, IL-2, and TNFa were also of interest. To streamline our panel and minimize errors in compensation, we designed three intracellular master mixes to specifically target their

corresponding T cell subsets (MM2 for Th1, MM3 for Th17, and MM4 for Tfh). This was achieved by maintaining consistency in the fluorophores used and conjugating them with the appropriate cytokine-specific antibodies as required.

Two FMOs (fluorescence minus one) were used under mock and PMA/ionomycin conditions. The plate was ordered left to right as follows: a negative control mock well containing cell media, a positive control well containing PMA/ionomycin (2µL/mL of cell media), a CEFX well (1µL/250µL of cell media), and a RBD well (1µL/250µL of cell media). This was replicated two more times creating a total of 12 wells. This created three groups of four wells with each group containing a different master mix to test for each T cell subset (ordered Th1, Th17, and Tfh from left to right). Each master mix contained their respective cytokine-specific antibodies diluted in Perm/Wash. These master mixes were withheld from FMOs and single stains but added to experimental wells. Master Mix 1 (MM1) contained FITC, APC-Cy7, and blocking solution and was used to identify T cells from gross PBMCs. MM1 was added to FMOs and experimental wells but withheld from single stains.

Once thawed, cells were resuspended to a concentration of 5E6/mL of cell media and were incubated under the same conditions as the ELISpot analyses overnight. The cells were once again resuspended to the same concentration (5E6/mL of cell media) and left to incubate for one hour. Afterwards, GolgiPlug (BD Biosciences, 555029) was added for an additional three hours at a concentration of 1µL of GolgiPlug to 1 mL of cell suspension. Cells were then washed and added to their platted conditions with 200 µL of FACS buffer. Following platting, cells were stained and fixed with appropriate incubations at room temperature and washes in between steps.

Each well received 50µL of blocking solution (50µL of FcX in 1mL FACS buffer) and 50µL of surface stain master mix solution was added to experimental wells and FMOs. Wells were resuspended in 100µL BD Perm/Fix solution and incubated protected from light (all subsequent incubations were done protected from light). Perm/Wash was used to rinse these wells and to resuspend during intracellular staining. Staining protocol ended with wells being resuspended in 200 µL of FACS buffer and sent for flow cytometry.

Figure 2: Flow Cytometry Gating Schematic

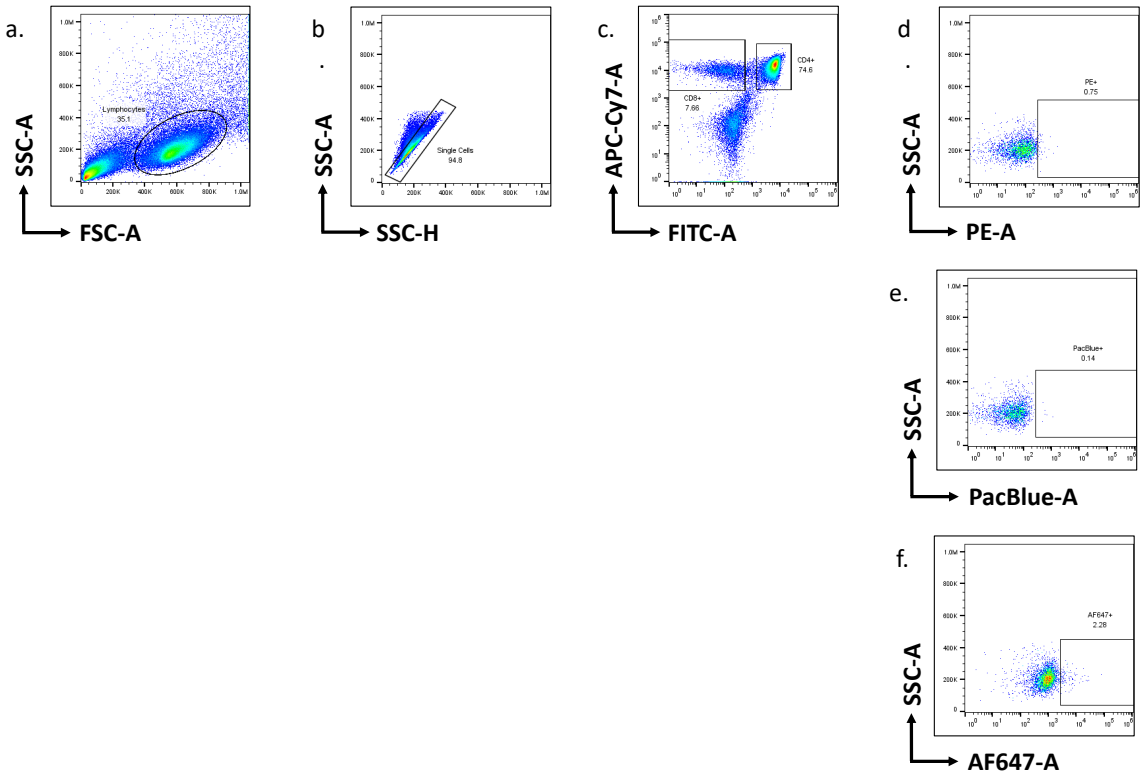

Gross PBMC's gated for lymphocytes using forward scatter (FSC) and side scatter (SSC) (**a**). Gated single cells from the parent Lymphocyte gate using side scatter width (SSC-W) and side scatter area (SSC-A) (**b**). CD4+ and CD8+ T cells gated from parent single cells using FIT-C (x axis labeled CD4) and APC-Cy7 (y axis labeled CD3) (**c**). Gating of CD4+ PE, PacBlue, and AlexaFluor647 (**d, e, f**).

3.3 B cells

3.3.1 Qualitative Approach to Neutralizing Antibody Titers

Percent inhibition was determined in our investigations using a standardized protocol provided by GeneScript to analyze neutralizing antibody titers to the SARS-CoV-2 RBD. All materials and reagents were derived from GeneScript's SARS-CoV-2 Surrogate Virus Neutralization Test Kit (GeneScript, L00847). To start, concentrated wash buffer was warmed to 37°C to ensure the dissolution of any precipitate, while the rest of the kit components were kept at room temperature. Serum samples were briefly thawed then centrifuged to ensure sample homogeneity. Samples were diluted 1:10 in standard buffer, along with the blank, positive, and negative controls from the kit. RBD-HRP (GeneScript, Z03594) was also diluted at a 1:1000 in HRP dilution buffer. For each sample, a neutralization reaction was assembled by combining the diluted serum with RBD-HRP in a 96-well plate, followed by a 30-minute incubation at 37°C. Afterward, the capture plate was prepared, and samples were transferred for a 15-minute incubation. Wash steps were performed with the original wash buffer and the kit's TMB solution (GeneScript, B00022) was added. This reaction was halted at the end of incubation through stop solution. Plate readings were taken at 450 nm on a Tecan plate reader.

Figure 3: Percent Inhibition Calculation with Interpretation

$$Percent\ Inhibition = \left(1 - \frac{OD\ Value\ of\ Sample}{OD\ Value\ of\ Bagkround}\right) \cdot 100$$

SARS-CoV-2 Neutralizing Antibody Test	>= 30%	Positive	SARS-CoV-2 neutralizing antibody confidently detected
	< 30%	Negative	SARS-CoV-2 neutralizing antibody not confidently detected

Equation used to calculate percent inhibition in neutralizing antibody assays (**top**) with interpretation of results (**bottom**). "OD" refers to optical density which is recorded by the 450nm Tecan plate reader.

3.3.2 Quantitative Approach to Neutralizing Antibody Titers

In our quantitative investigation, we employed a separate protocol from the same kit as our qualitative assay to assess neutralizing antibody titers across serial dilutions. We initially warmed the concentrated wash buffer (same as previous kit) to 37°C to facilitate the dissolution of any precipitate. The remaining kit components were maintained at room temperature, while an aliquot of the monoclonal antibody (mAb) standard was placed on ice to thaw. Serum samples were briefly thawed at 37°C, followed by vortexing for homogeneity and centrifugation at approximately 300xg for about 30 seconds to ensure proper settling.

A serial dilution series was conducted starting with an initial 1:10 dilution in sample dilution buffer. The series included up to five additional 1:3 dilutions, with each dilution being performed in singlicate wells. The sequence of dilutions was as follows: 1:10, 1:30, 1:90, 1:270, 1:810, 1:2430. Positive and negative controls from the kit were also diluted 1:10 with sample dilution buffer, with duplicates receiving 14 µl of control and 126 µl of sample dilution buffer. To prepare the mAb standard curve, we first created a diluted stock of mAb at 3 µg/ml. Subsequently, this stock was used to generate a series of working solutions, following a specified dilution pattern. RBD-HRP (same as previous protocol) was diluted 1:1000 by adding 10 µl of RBD-HRP concentrate to 10 ml of HRP dilution buffer.

For the neutralization reaction, 60 µl of each diluted serum sample was mixed with 60 µl of the RBD-HRP solution for singlicate samples, while duplicates received 120 µl of each. This reaction took place in a 96-well plate, with a maximum total volume of 240 µl per well. The plate was covered with foil and incubated for 30 minutes at 37°C. Wash buffer was prepared by adding 40 ml of 20x concentrate to 760 ml diH2O. Subsequently, 100 µl of each "neutralized"

sample was transferred to the capture plate according to the plate layout, and the plate was again covered with foil and incubated for 15 minutes at 37°C. The capture plate underwent four wash cycles, each using 260 µl of wash buffer. After each wash, the plate was blotted on paper towels and thoroughly dried after the fourth wash. Following the wash steps, 100 µl of TMB solution was added to each well, and the plate was covered with foil and incubated in the dark for 15 minutes at room temperature on a rocker. To conclude the assay, 50 µl of Stop Solution was added to each well. Plate readings were immediately taken at 450 nm on a Tecan plate reader, including initial shaking to ensure proper mixing of the stop solution.

At this time, no data is available from this quantitative approach to supplement the qualitative data we have generated. These assays are still being performed as of the date of this publication and updates of results/findings will be uploaded accordingly.

Results

T cell INFy Production Minimally Impacted by Immune Therapy Against SARS-CoV-2

IFNy has been shown to be decreased in immunosuppressed and immunocompromised individuals, however, examination into the downstream effects, particularly in the instance of a pathogen introduction, have not been investigated until now[38,39,40]. It was important for us to first evaluate the relative T cell fitness of immunosuppressed individuals compared to their healthy control counterparts before identifying T cell subsets. We achieved this through an in vitro ELISpot assay sensitive to INFy production. Upon exposure to the CEFX and RBD peptide mixes, the lymphocytes would secrete INFy and implant to the well's substrate inducing a "spot"

on the plate. There does not appear to be a biologically or statistically significant difference between immunosuppressed patient and healthy control IFNy production in both the CEFX condition and the RBD condition. When comparing subject (both healthy and patient) responses between CEFX and RBD, most CEFX responses showed spot production levels that were 1 to 6 folds higher than those observed when exposed to RBD. Patients and healthy controls alike show a great deal of variance within their respective groups in their IFNy response to the CEFX peptide mix with standard deviations being quite comparable (149 for healthy controls, 140 for rituximab patients, and 203 for MMF patients) (Fig. 4). Rituximab-treated patients appear to mimic their IFNy responses with healthy controls while MMF-treated patients appear to be dichotomized into two distinct groups (one impressively high and one impressively low). Patients and healthy controls alike mount a minute INFy release when responding to the RBD peptide with the means of 18, 32, 27 from the same three subject groups respectively. Standard deviations in response also vary minimally with most subjects remaining within a few ten spots of the calculated means (21, 44, 17 per group respectively).

Figure 4: T Cell Responses to CEFX and RBD at V1 Timepoint

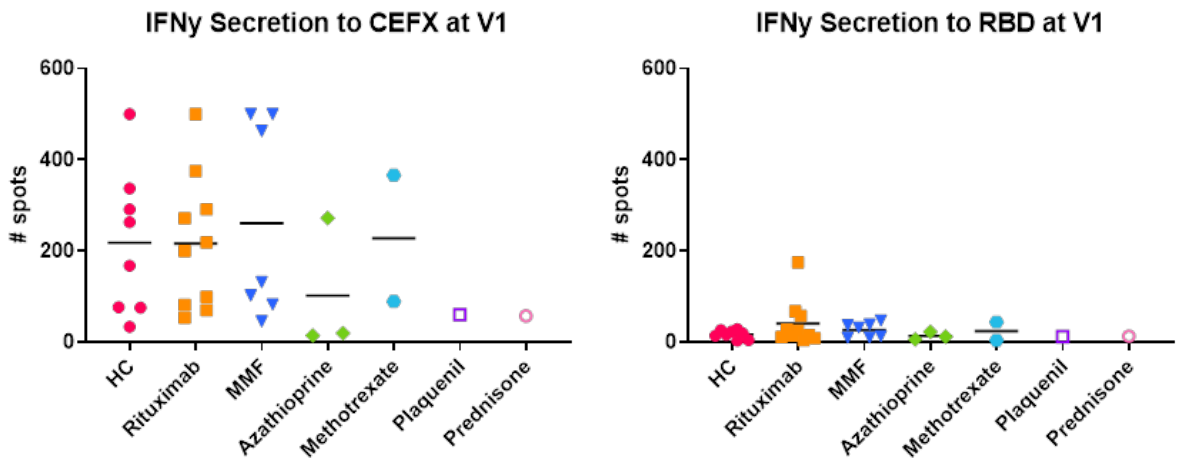

Cumulative CEFX data from V1 ELISpots (**left**) compared to cumulative RBD data taken from the same V1 ELISpots (**right**). Horizontal bars in both graphs represent the means of each columns' data. For data with only one sample (Plaquenil and prednisone), samples were denoted as a single point with no mean bar.

To properly assess RBD spot responses at V1 among vaccine recipients, we expanded these points through decreasing our y axis metric from 600 spots to 100 spots (Fig. 5 Left). The general trends seen in subject CEFX responses can be seen in the RBD, as well. Rituximab-treated patients show relatively similar results to healthy controls and MMF-treated patients appear to be dichotomized into impressively high and impressively low groups. We proceeded to normalize subject RBD responses by calculating their RBD/CEFX ratios (Fig. 5 Right). These ratios for healthy controls on average hover just above zero (meaning there was no RBD response which would nullify any CEFX response in this display) for healthy controls at the V1 timepoint while patients, remarkably, show higher RBD responsiveness even given their reduced immune fitness. With this increased mean, though, there is an even greater margin of error with patients having more variable responses versus their healthy counterparts.

Figure 5: T Cell Responses to RBD Expanded and RBD/CEFX Ratios at V1 Timepoint

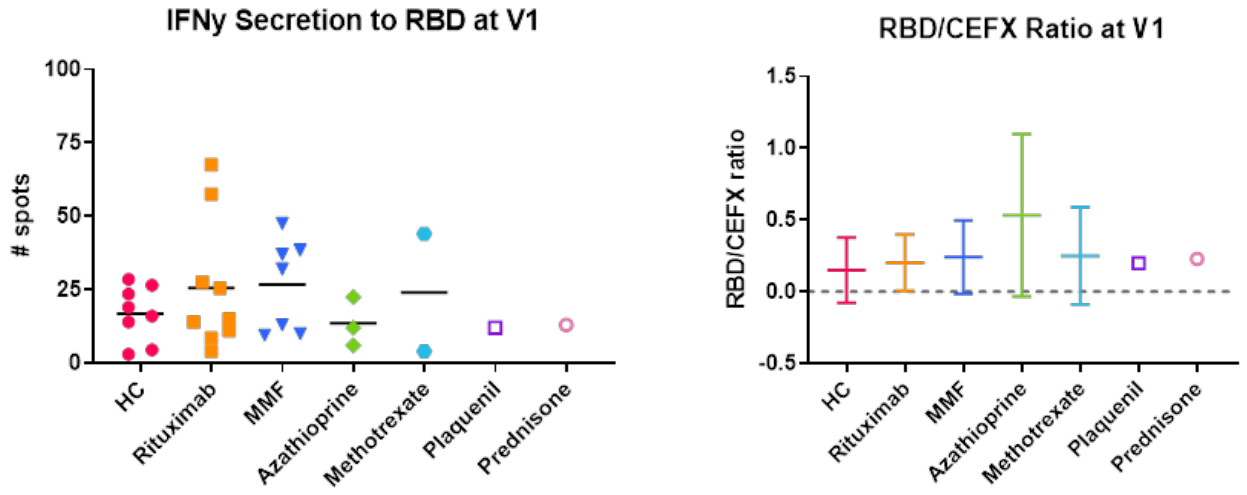

Cumulative RBD data from the same V1 ELISpots expanded to a y axis range of 0 to 100 spots to highlight distinct individual T cell responses (**left**). Horizontal bars represent the means of each columns' data. For data with only one sample (Plaquenil and Prednisone), samples were denoted as a single point with no mean bar. The RBD/CEFX ration was calculated as the number of spots in the RBD wells per the number of spots within the CEFX wells per patient (**right**). Horizontal bars represent the mean for each columns' data along with error bar. Dotted line marks an RBD/CEFX ratio of "0" across the horizontal plane.

We further wanted to examine longitudinal RBD responses on an individual-by-individual basis with each line correlating to a patient over the course of the study (Fig. 6). More samples were run at these various timepoints, however, only samples tracked over at least two timepoints were eligible for this plot. Healthy controls and rituximab-treated patients alike show a remarkably similar trend among their respective cohorts. A dip in RBD spots can be viewed in these two groups between the V1 and V2 timepoints with an increase only occurring upon receiving the BV1 updated vaccine against the Delta strain of the virus. Also of note is the fit each of these groups have among their respective individuals with healthy controls maintaining the strongest correlation to their trendline (variance of 1.38 at V0, 66.06 at V1, and 35.30 at V2)

compared by rituximab-treated patients (variance of 2517.12 at V1, 2328.06 at V2, and 82.06 at BV1). The final longitudinal plot of miscellaneous therapies possesses the least amount of correlation (variance was not calculated and was remarked as such from visual observation).

Figure 6: Longitudinal ELISpot Data Across All Timepoints

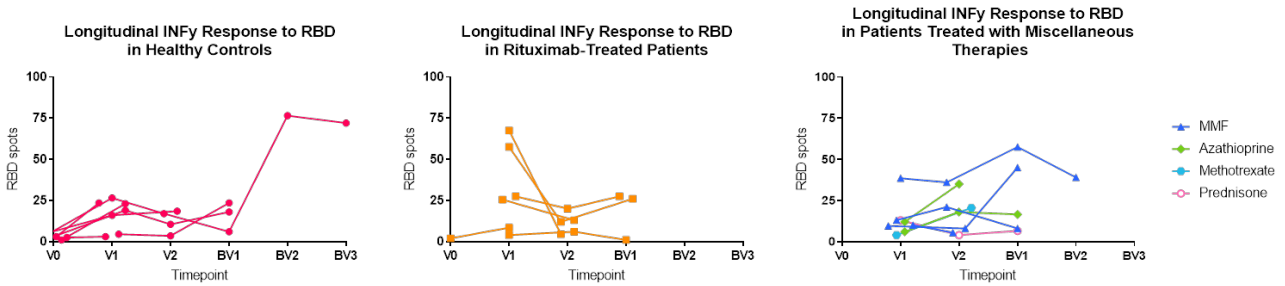

Number of RBD spots elicited by subject T cells over the course of all timepoints with lines connecting samples retrieved from the same subject (**left**). The same plot as the left modeled instead using immunosuppressed individuals undergoing rituximab treatment (**center**). The same plot as the left modeled instead using immunosuppressed patients undergoing MMF (**blue triangle**), Azathioprine (**green dot**), Methotrexate (**blue hexagon**), or Prednisone (**pink hollow dot**) (**right**).

Patient T cell Subsets Functional with Exacerbated Cytokines Compared to Healthy Individuals

The demographics of lymphocyte subsets hold significant importance not only for immunosuppressed patients but also for the broader community. Lymphocyte subtypes are critical in ensuring a proper immune repertoire is present to protect an individual[41,42]. The immune cell types and their relative numbers has been an area of intense scrutiny as deficiencies and abundances of these subsets are often directly related to the pathology of vast autoimmune disorders[43]. Of importance to our research question, we investigated Th1, Th17, Tfh, and CD8 T cell numbers indirectly through their cytokine release milieus. Flow cytometry

showed a global (for all subjects) increase in cytokine release from V1/V2 to BV2/BV3 timepoints (Fig. 8). Healthy controls and immunosuppressed patients present with relatively similar cytokine concentrations. A visible variance can be found between healthy controls and our three immunosuppressed cohorts, however, we found these variances to be minimally impactful to overall immunity. These variances are expressed as percentages of percentages, resulting in an extremely marginal compounded difference. In all, these results showed that T cell cytokine production was minimally impacted to a biologically or statistically significant level. T cell subsets do not appear to be impaired in their ability to protect their immunosuppressed individual from the SARS-CoV-2 virus compared to healthy controls.

Figure 7: Cumulative Flow Cytometry Data By Timepoint, By Therapy, By Subset, By Well Plate Condition, and By Cytokine

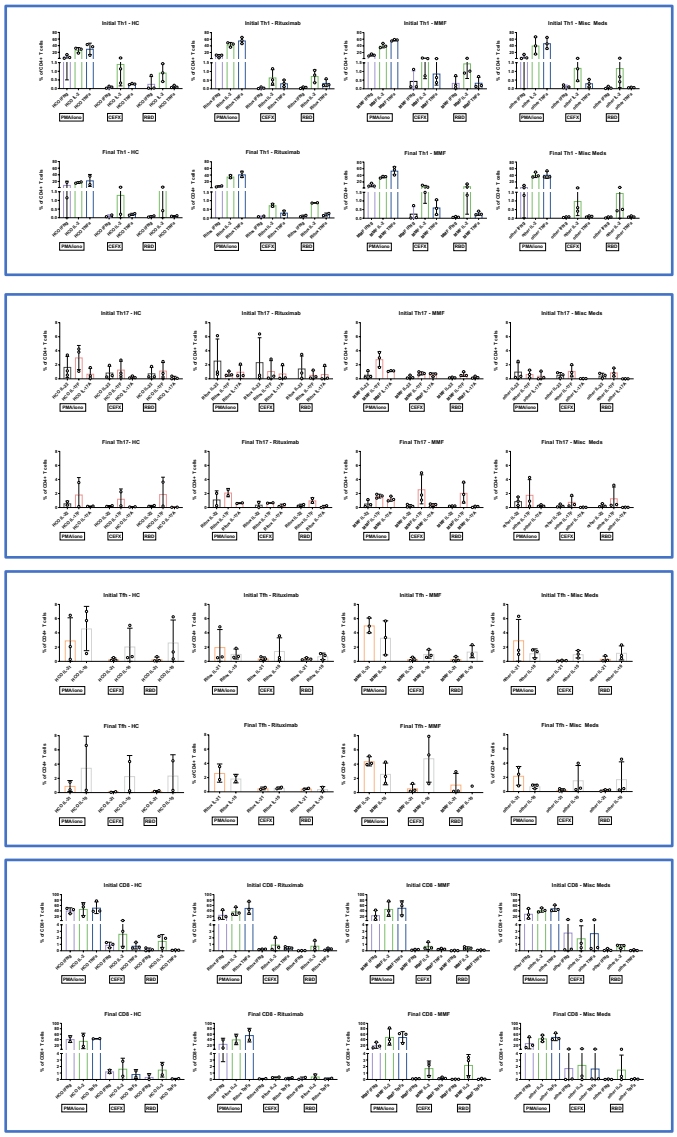

T cell subsets were measured indirectly by their cytokine release milieus. Each graph is structured by displaying the mean with error bars for each cytokine. Well plate conditions are modeled per graph from left to right: PMA/ionomycin, CEFX, and RBD. The x axis labels the cytokines and the y axis represents the % of the parent gate they occupy. Graphs are separated horizontally by healthy controls (**far left**), rituximab-treated patients (**center left**), MMF (**center right**), and patients treated with other medications (**far right**). Graphs are separated vertically per graph by V1/V2 responses (**top**) and BV2/BV3 responses (**bottom**). Cytokines are color-coded according to Graphic 4's legend. **A.** Th1 cells identified by IFNy (written synonymously as "IFNg" above, **purple**), IL-2 (**green**), and TNFa (**blue**). **B.** Th17 cells identified by IL-17A and IL-17F (**salmon**) along with IL-22 (**dark grey**). **C.** Tfh cells identified by IL-21 (**peach**) and IL-10 (**light grey**). **D.** CD8 T cells identified by IFNy (**purple**), IL-2 (**green**), and TNFa (**blue**).

Across all T cell subtypes, both healthy controls and immunosuppressed patients increased cytokine release during their BV2/BV3 timepoints compared to their V1/V2 timepoints. Healthy controls tended to perform most appropriately and often higher than their immunosuppressed counterparts. Patients taking MMF, however, tended to produce inappropriate responses and often performed highest (even higher than their healthy control counterparts) during their BV timepoints. Another trend to note is the change in cytokine ratios by T cell subtype. Upon analyzing healthy control and patient BV timepoints, IL-2, IL-17F, and IL-10 were much higher compared to their respective sister cytokines within their respective milieus.

Figure 8: Cumulative Flow Cytometry Data Simplified to Relative T Cell Subset Population Sizes Over Time

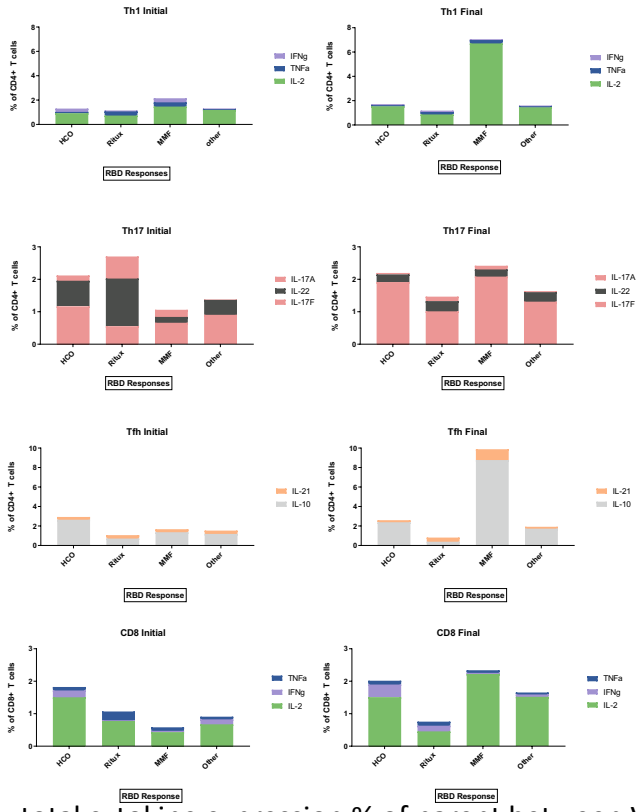

T cell subsets quantified by total cytokine expression % of parent between V1/V2 and BV2/BV3 timepoints. Cytokines retained their color-coding from previous figures and graphics. Bar graph color-coding should be read from top to bottom which matches their respective graph's legends' order. **A.** Th1 cumulative cytokine expression in response to RBD peptide mix in healthy controls, rituximab-treated patients, MMF-treated patients, and patients treated with other medications. **B.** Th17 cumulative cytokine expression in response to RBD peptide mix in healthy controls, rituximab-treated patients, MMF-treated patients, and patients treated with other medications. **C.** Tfh cumulative cytokine expression in response to RBD peptide mix in healthy controls, rituximab-treated patients, MMF-treated patients, and patients treated with other medications. **D.** CD8 cumulative cytokine expression in response to RBD peptide mix in healthy controls, rituximab-treated patients, MMF-treated patients, and patients treated with other medications.

Though the demographics of T cell subsets appeared relatively equal between healthy controls and immunosuppressed patients, the individual cytokine levels were released in different magnitudes between these groups. Healthy controls demonstrated a normal increase of cytokine production between a 0.25 and 1.8 fold increase while patients often had certain

cytokines released at an inappropriate amount. Notably, rituximab-treated patients saw a robust increase in CD8 IFNy production and MMF-treated patients saw a robust increase in Th1 IL-2, Th17 IL-17F, Tfh IL-10 and IL-21, and CD8 IL-2.

Figure 9: Final/Initial Ratios of T Cell Cytokines

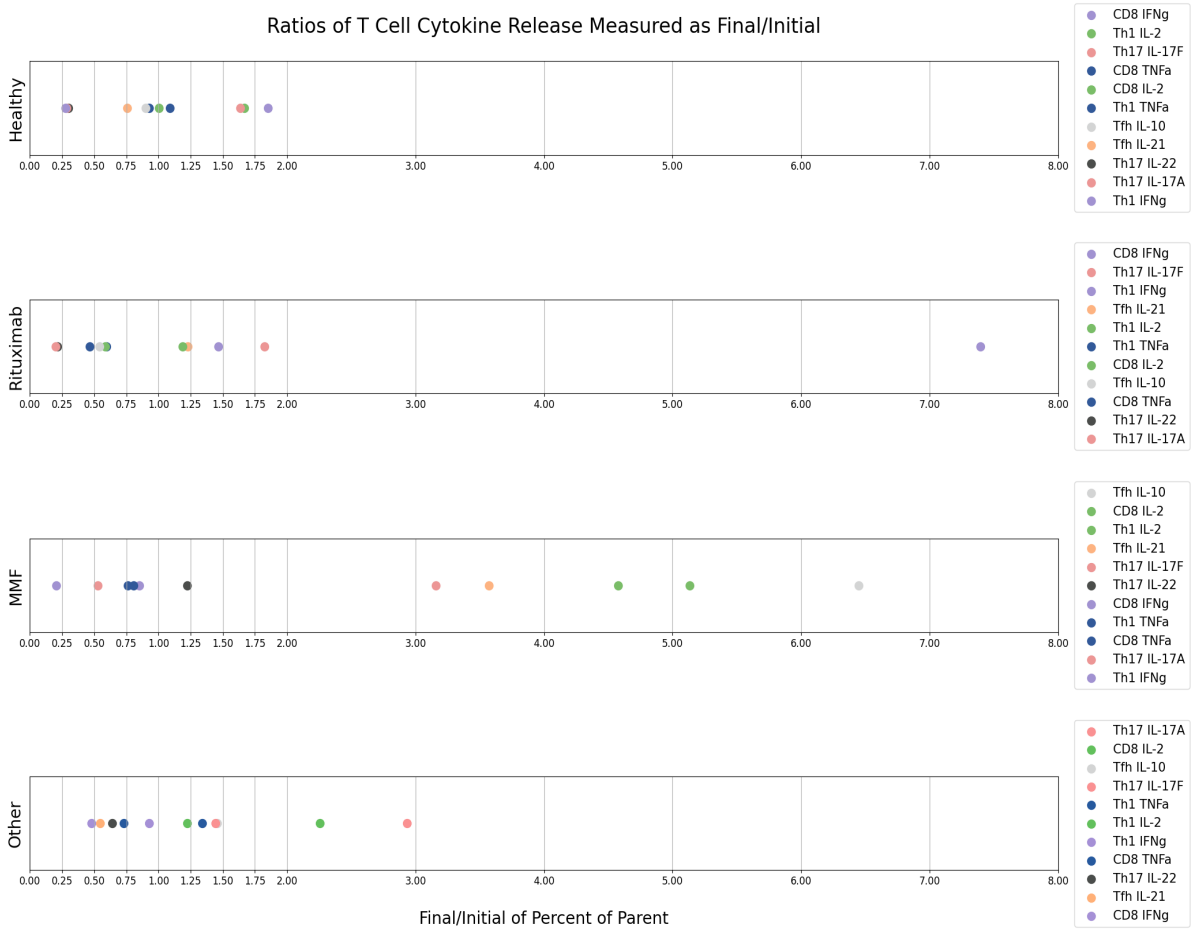

Final cytokine percent of parent over initial cytokine percent of parent in response to the RBD peptide graphed on a linear continuum. Legends correlate to the highest value on the number line (top cytokine on legend) trending towards the lowest value on the number line (bottom cytokine on legend). Thus, the legends are different for each of these graphs as they are sorted for their respective conditions. Continuum conditions include healthy individuals (**top**), rituximab-treated patients (**second from top**), MMF-treated patients (**third from top**), and "Other" representing the miscellaneous medications as previously stated in previous analysis (**bottom**). Horizontal increments of each continuum are marked in 0.25 intervals until "2.00" in which intervals are then marked in 1.00 increments.

Patient B cell nAb-Associated Percent Inhibition Stratified by Unidentified Indicator

Current literature on the humoral response elicited by immune compromised individuals to the SARS-CoV-2 antigen protected solely by vaccine has not yet been canonized concretely. Results from various research groups have proposed contradictory results likely due to what we describe as an unidentified indicator of humoral efficacy. We conducted numerous ELISAs geared towards measuring neutralizing antibodies to the RBD peptide of the SARS-CoV-2 virus. From this, we calculated an individual's percent inhibition along the timepoints of our study. We found a decrease in percent inhibition occurred between the V1 and V2 timepoint that was then quickly recovered at the BV1 timepoint. Following booster vaccination (BV1), patient percent inhibition continued to trend upward steadily through the end of our study. Patients greatly varied in antibody response across all timepoints with select patients performing well (*adequate*, high percent inhibition), performing moderately and variably (*moderate*, intermediate), and poorly (*inadequate*, low percent inhibition). We demonstrated three trends of great importance to our research question: antibody production waned between V1 and V2 timepoints, booster vaccination induced a drastic increased production of neutralizing antibodies which continued to increase as time progressed, and patient percent inhibition could be grouped into three relative groups.

Figure 10: Percent Inhibition of Longitudinal Patient Neutralizing Antibody Titers

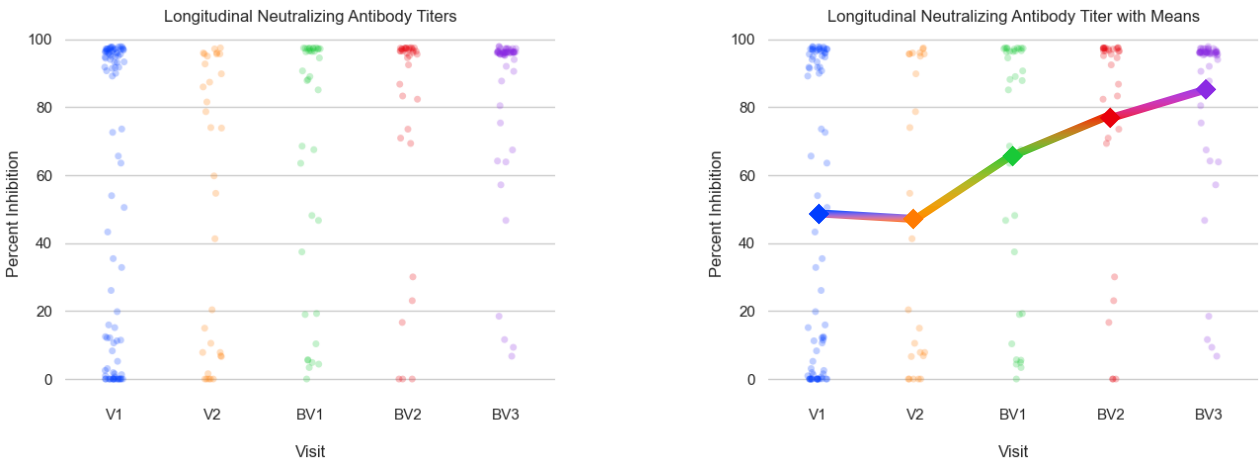

Percent inhibition achieved by patient B cell neutralizing antibodies against the SARS-CoV-2 virus' RBD peptide through in vitro ELISA. Each dot corresponds to a single sample. "Visits" are highlighted on the x axis as V1, V2, BV1, BV2, and BV3 to show longitudinal neutralizing antibody efficacy. Colors are meant to differentiate visit to visit and hold no need for legend. A decreased opacity was chosen to display clustering and density of dots in various regions. Means per timepoint are denoted as diamonds with linear lines connecting them as a pseudo-trendline (**right**). Means are removed with the raw data uninterrupted (**left**).

We chose to proceed with our data analyses by properly characterizing the three groups we visually identified. Our intuition was confirmed by a k-means clustering algorithm of our data which showed three distinct clusters across all five timepoints. These clusters occupied the ranges of 0 percent inhibition to 21 (Cluster 1), 22 to 74 (Cluster 2), and 75 to 100 (Cluster 3). We subsequently evaluated patients which occupied each of these clusters at the V1 timepoint compared to their BV3 timepoint to see their longitudinal progress. We saw that while most individuals performed significantly higher following booster vaccination than following their initial dose/s, some which occupied Cluster 1 at V1 never exceeded the 21% inhibition threshold. Additionally, some individuals who performed highly and occupied Cluster 3 at V1 experienced a decrease in percent inhibition. This has led us to believe that an indicator exists which could explain these stark trends.

Figure 11: Longitudinal Cluster Analysis of Patient Percent Inhibition Through Neutralizing Antibody Titers

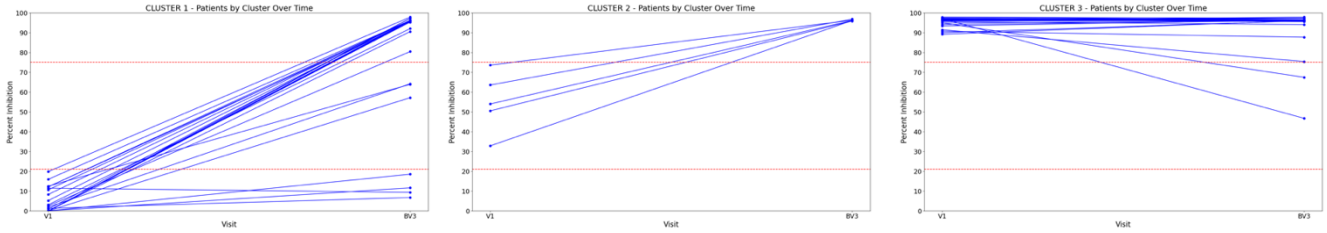

Patient percent inhibition values were subjected to k-means clustering at V1, V2, BV1, BV2, and BV3 timepoints to identify the ideal number of clusters and ranges to classify them. Three clusters were identified at each timepoint and the cutoffs for each are denoted by a horizontal red dashed line. “Cluster 1” was identified to be percent inhibition values of 0-21, “Cluster 2” 22-74, and “Cluster 3 “75-100. Cutoffs were set at 21 and 75 respectively. Long-term changes in percent inhibition are tracked per patient with a line correlating to their V1 and BV3 response. Graphs are arranged left to right as Cluster 1, Cluster 2, and Cluster 3

We further generated longitudinal scatter plots to determine if an indicator could be elucidated by a single demographic. Patient therapy, disease involvement, age, race, body mass index (BMI), vaccine formula, and cluster were identified as demographics of high interest. Evaluation of all seven demographics yielded no result. This left our group with the deduction that either another primary indicator exists which we have not yet identified or that there is a combination of secondary indicators which contribute to the trends we previously identified.

Figure 12: Percent Inhibition of Longitudinal Patient Neutralizing Antibody Titers By Demographic of High Interest

Patient percent inhibition of B cell produced neutralizing antibody titers over the five major timepoints of the study differentiated by demographic. Graphs can be read left to right, top to bottom as “Therapy”, “Disease Involvement”, “Age”, “Race”, “BMI”, “Vaccine Formula”, and “Cluster”. The same color pallet was used for each graph per the graphs programming, however, each graph should be read isolated from the rest. The legend for each graph is highlighted below its respective plot.

We, finally, desired to look at all three clusters together longitudinally. From this view, we deduced that initial vaccine responses were dichotomized primarily into either *adequate* (Cluster 3) or *inadequate* (Cluster 1). These two groups, however converged at BV3 with a majority of patients achieving *adequate* protection.

Figure 13: Complete Longitudinal Tracing of Patient Percent Inhibition Through Neutralizing Antibody Titers

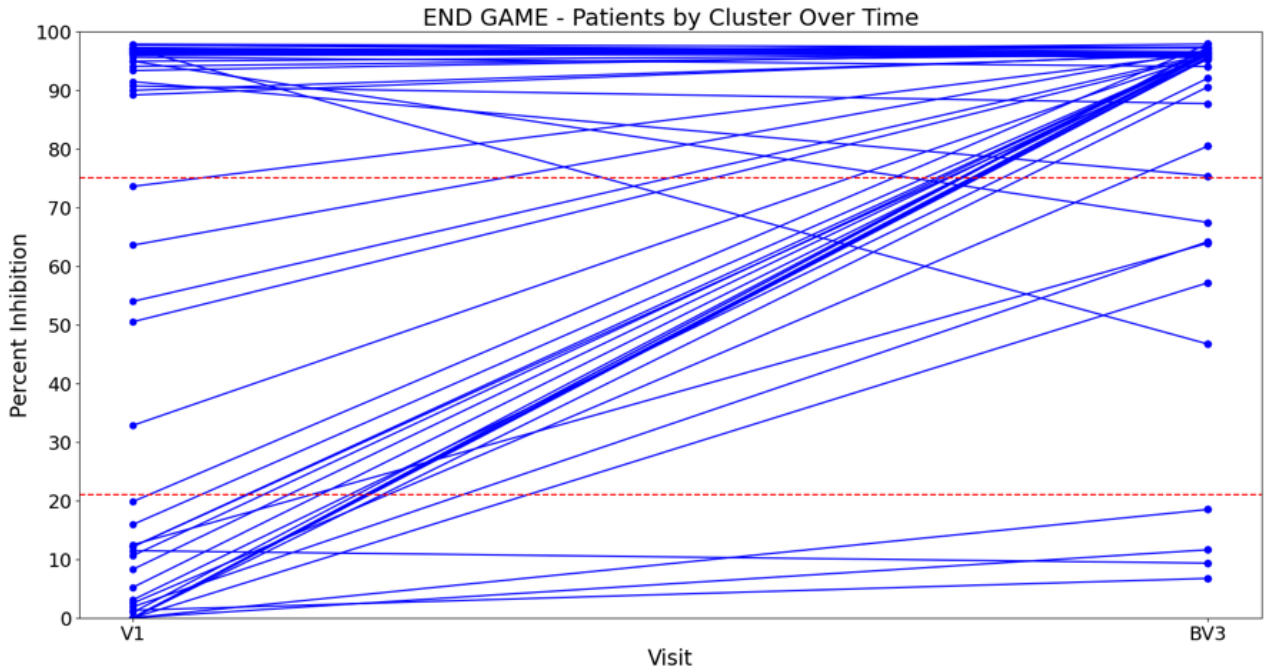

Cumulative neutralizing antibody percent inhibition data per patient are denoted by dots at their timepoints with a line connecting them as a trendline. Trends were established from initial timepoint (V1) to final timepoint (BV3). Clusters from k-means clustering analysis can still be distinguished by their horizontal dashed red line cutoffs.

Discussion

T Cells Decrypted

The T cell arm of our study yielded results indicating to us that T cell performance was minimally impaired by patient immunosuppressive therapy. We found CEFX helpful in gauging

patient immune fitness by providing a reliable standard to normalize T cell response values to the RBD peptide. Samples (both healthy controls and patients) procured from the V1 timepoint had egregiously low responses to the RBD peptide particularly when compared to their response to the CEFX peptide mix. There was between a 1 to 6 fold difference in CEFX response compared to RBD response. We believe this can be explained due to the frequency in which subjects have encountered the pathogens present in the CEFX compound (clostridium tetani, human herpes virus, influenza A, measles, rubella, toxoplasma gondii, among others) compared to the novel corona virus. There is no standard as provided by the kit or in the literature to denote a strong versus weak IFNy response from these ELISpots, however, we find less than 100 spots from RBD stimulation to be incredibly low particularly when examined next to CEFX responses. This further emphasizes the importance of vaccine protection as well as proper understanding of how individuals are protected from malicious pathogens especially given the future predicted propensity for more pandemics to occur[43].

When examining RBD/CEFX ratios, patients demonstrated relatively results to healthy controls which was additionally contrary to our initial hypothesis. Upon further examination into the RBD/CEFX ratios, CEFX response appeared to primarily drive the ratio. It was also interesting to note during this anecdotal investigation that there was a not a clear correlation between a high CEFX response and high RBD response or vice versa. Some patients, as well, were found to pose stronger responses to the RBD peptide mix than their healthy control counterparts which could be an interesting tangent to elucidate in the future.

When investigating longitudinal IFNy release, individual healthy controls displayed a strong correlation and low variance among each other compared to patients. Both the

rituximab group and miscellaneous medication group showed high levels of variation patient-to-patient, however, do display a rough trend of increased IFNy release following the booster vaccine (BV1). Both patients and healthy controls show a depression between the initial follow-up visit (V1) and second (V2) that only rises upon booster (BV1) administration. This confirms current documentation found in the literature indicating the importance of the booster vaccine in maintaining immunity against the ever-evolving SARS-CoV-2 virus[45].

Though IFNy production did not differ between patient and healthy control, we did find that in certain instances either patient immunotherapy and/or underlying condition elicited an inappropriate cytokine response to the RBD peptide mix. Upon gross cytokine analysis of subject T cells, all groups showed an increase in cytokine release following the BV timepoints with MMF maintaining the highest response rate – even greater than healthy controls. We hypothesize that this could be the visualization of a virus-induced cytokine storm within these patients. These T cells seem to be engaged in irresponsible cytokine activity that could be related to their pathology and their necessity for MMF as their treatment. This, too, is actively being investigated by our team. Aside from this finding, another finding of interest to us is the increase in IL-2 in Th1 and CD8 T cells, IL-17F in Th17 cells, and IL-22 in Tfh T cells at healthy control and patient BV timepoints. This shows T cells are having a proper robust response to the RBD peptide due to an enhanced immune response following sufficient vaccination doses.

B Cells Decrypted

The starkest evaluations we found were within the B cell arm of our investigations. We found in our qualitative investigations of patient neutralizing antibody percent inhibition that

there appears to be either a primary or multiple secondary demographics which could form an indicator and predictor of patient nAb production. Patient percent inhibition data subjected to our k-means clustering algorithm ideally grouped our data points into three clusters: Cluster 1 with 0 to 21 percent inhibition, Cluster 2 with 22 to 74 percent inhibition, and Cluster 3 with 75 to 100 percent inhibition. All patients in Cluster 2 (*moderate*) at V1 reached Cluster 3 (*adequate*) by the BV3 timepoint and most patients from Cluster 3 at V1 remained as such until BV3. Some patients, however, dropped from Cluster 3 to Cluster 2. Likewise, most patients identified in Cluster 1 (*inadequate*) at the V1 timepoint were successful over the course of the study to produce neutralizing antibody responses to achieve Cluster 3 status by the BV3 timepoint. Some patients, however, never achieved higher than 21 percent inhibition which is troublesome as responses below 30% are considered invalid by GeneScript's kit's standards. We are unsure at this time the reason behind this trend. We are currently invested in determining why certain patient percent inhibition decrease longitudinally as well as why some never exceed the 30% threshold.

We focused our investigating next towards what demographics could act as a reliable indicator of patient cluster assignment, more specifically, their percent inhibition. We identified patient immunosuppressive therapy, disease involvement, age, race/ethnicity, BMI, vaccine formula, and cluster assignment as promising indicators in descending perceived importance. We were unsuccessful in identifying a primary indicator from this methodology which has led us to alter our hypothesis that multiple secondary demographics could act as an indicator and predictor. A more likely hypothesis we are operating under, however, is the belief this indicator is correlated to patient immunosuppressive therapy administration schedule. Compared to

healthy controls (both of our own personal analyses and of literature analyses), patients demonstrate a wider variability in their response to the vaccine. This, we are confident, is due to patient immunotherapy, in part. Ultimately, evidence was not found to confirm or deny these hypotheses and are both ongoing interests of our team.

Clinical Application

Given our belief that immunosuppressive therapy schedule is altering patient B cell ability to mount a proper immunity to the SARS-CoV-2 RBD peptide, we are working diligently to determine where in the humoral pathway therapies are disrupting. Given the data we have

Graphic 5: The Chicken, The Egg, & The Omelet

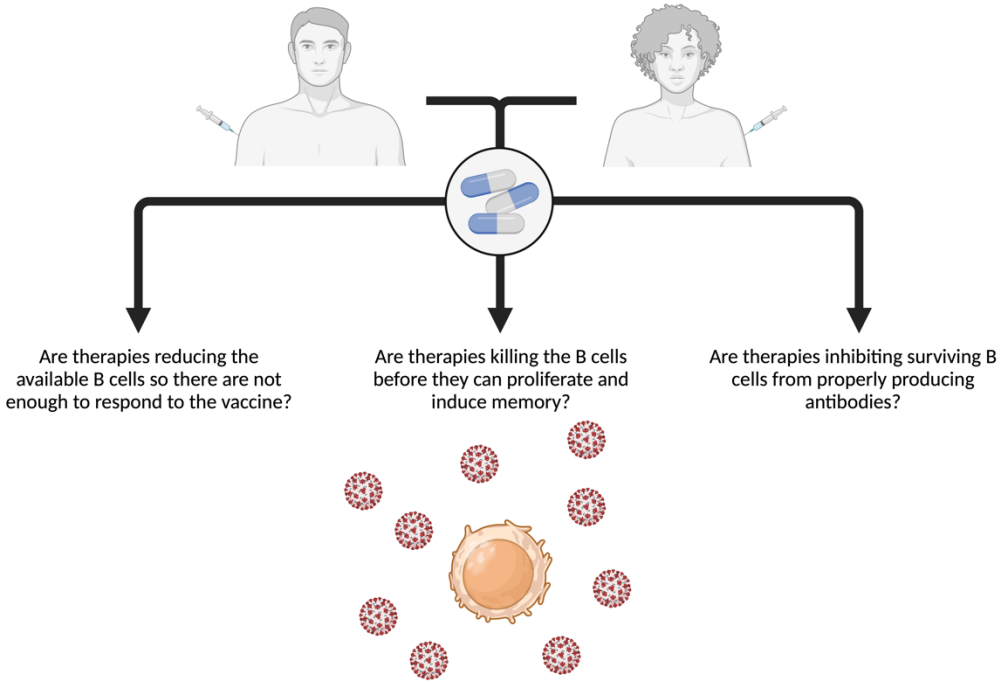

Illustration of our current theories into how B cells are being impacted by patient immunosuppressive therapy. The “Chicken” hypothesis infers that B cells are unable to respond to the vaccine due to decreased numbers. The “Egg” hypothesis infers that B cells are unable to proliferate and induce memory to the SARS-CoV-2 antigen. The “Omelet” hypothesis infers that B cells are being eliminated at the time of infection preventing their ability to mount a proper antibody response.

produced, we are left with what came first: the chicken, the egg, or the omelet. This is obviously a play on the age-old adage; however, it proves as a good thought experiment to present the three hypotheses we have generated.

Hypothesis 1 – The Chicken

The hypothesis which would occur first chronologically would be that patient therapies are reducing the available B cells so there are too few to properly respond to the vaccine when administered. Should this be the case, it would be recommended for physicians to:

1. Regularly monitor patient B cell counts (which is already practiced) to assess the impact of therapies on their levels and adjust therapies as needed to prevent a significant depletion of B cells.
2. Adjust therapy administration, if possible, to avoid coinciding with vaccination schedules in hopes of maintaining an adequate B cell number for a vaccine response.
3. Consider alternative therapies or treatment options that pose a less pronounced depletion of B cells while still effectively managing the patient's condition.
4. Offer immunoglobulin replacement therapy in cases where B cell levels are critically low to provide patients with the necessary antibodies to respond to infections, including vaccines.

Hypothesis 2 – The Egg

The next logical hypothesis would be that patient therapies preferentially target B cells and are doing so while they attempt to proliferate, thus, impeding the patient’s immune system

from inducing B cell memory. Should this be the case, it would be recommended for physicians to:

1. Provide immune support geared towards surplus generation of B cell memory. This may manifest as supplemental vaccines, booster vaccinations, or specific interventions to enhance B cell memory formation.
2. Explore therapies which can be tailored to minimize interference with B cell memory formation.
3. Proceed with therapy administration adjustment, alternative therapies, and/or IV Ig treatments as stated in Hypothesis 1's points 2, 3, and 4.

Hypothesis 3 – The Omelet

The final possible hypothesis would be that patient therapies inhibit B cells constitutively from properly producing antibodies. Should this be the case, it would be recommended for physicians to:

1. Consider the use of monoclonal antibodies or other treatments to compensate for the impaired antibody production in the patient (as stated both in Hypothesis 1 and Hypothesis 2).
2. Explore alternative treatments that have a proven lower impact on B cell antibody production while effectively managing the patient's underlying condition.
3. Regularly monitor patient desired epitope-specific antibody levels and adjust therapies accordingly.

4. Investigate immunomodulatory therapies to fine-tune the patient's immune system and promote more effective antibody production.

These hypotheses do not have to be mutually exclusive and can all be actively occurring within the periphery of immunosuppressed patients. This is a line of further questioning which is necessary to determine if clinical adjustments should and can be made.

Limitations and Future Directions

Though this study provides many incredible findings which can and should spawn future investigation, it is important to note the limitations of this research's application. Humans are unlikely to be ideal subjects for our study aims due to the multitude of variables that must be accounted. Variables such as naturally acquired COVID-19 infection (whether known or unknown to the subject), comorbidities (which would impact a subject's immune fitness), the rapidly evolving nature of the virus, and the lack of continuous refinement of commercial antibodies and assays.

The Falk Lab and UNC Kidney Center wishes to take this research a step further in elucidating conclusions from these results. Future directions for the lab include:

I. Identifying RBD-specific T cells through tetramer assays
II. Evaluating our patient data at a much smaller scale through eliminating extraneous variables and focus solely on patients experiencing ANCA-associated vasculitis and undergoing Rituximab treatment as this was our largest patient cohort

III. Cross-referencing date of rituximab treatment with date of vaccination and date of sample procurement (essentially monitoring treatment administration schedule alongside vaccination schedule)

IV. Examining the profile information on the eight patients from V1 Cluster 1 and the four patients from V1 Cluster 3 which performed worse in BV3 to identify a correlating variable

V. Complete our quantitative analysis of patient neutralizing antibody titers across an extensive dilution series to compare percent inhibition from qualitative assays to effectiveness of the epitopes developed by patient B cell antibodies

VI. Complete a multiple linear regression on patient variables and interpret through residual plots to identify the highest predictors of antibody production quality and quantity

Conclusion

The significance of immunosuppressed individuals as a vulnerable patient population has risen to the forefront of public health efforts, particularly in light of the 2020 Pandemic. Our lab contributed to the growing literature of vaccine-induced immunity and underscored the paramount importance of this area of study. We uncovered compelling evidence in our investigations suggesting that patient T cells remain remarkably resilient in the face of immunosuppressive therapy. Additionally, we found an unidentified indicator which we believe could serve as a significant predictor of B cell performance to future novel pathogens. This indicator introduces a present unpredictability in patient neutralizing antibody response, raising

concerns for patient safety in the interim. Our findings remain challenged by multiple uncontrollable variables which has pushed our group to limit the scope of our patient population for future directions. We remain committed to advancing the understanding of immunosuppressed individuals' immune responses, with a focus on elucidating the unidentified indicator affecting patient B cell function. Our ultimate aim continues to be to improve patient care, enhance public safety, and contribute to alleviating immunosuppression concerns amid the perpetual endemic.

Acknowledgements

I would like to acknowledge the Falk Lab's study coordinating team as well as the multitude of physicians for their recruitment of participants for this project. I would like to acknowledge Dr. Donna Bunch and her associates for their work in performing our B cell analyses and nAb titer assays. I would like to thank Sandy Elmore for her assistance in performing several assays, data analyses, and general support during this project. I would like to thank Dr. Ronald Falk for housing me as a research assistant for the duration of my undergraduate education at UNC Chapel Hill. Finally, and most important to me, I would like to thank Dr. Meghan Free for mentoring me as well as inspiring me to pursue a career in research.

References

1. Lavine, Jennie S., Ottar N. Bjornstad, and Rustom Antia. "Immunological characteristics govern the transition of COVID-19 to endemicity." *Science* 371.6530 (2021): 741-745.

2. Coccia, Mario. "COVID-19 pandemic over 2020 (with lockdowns) and 2021 (with vaccinations): similar effects for seasonality and environmental factors." *Environmental Research* 208 (2022): 112711.
3. Singson, Jason Robert C., et al. "Factors associated with severe outcomes among immunocompromised adults hospitalized for COVID-19—COVID-NET, 10 states, March 2020–February 2022." *Morbidity and Mortality Weekly Report* 71.27 (2022): 878.
4. Kunisaki, Ken M., and Edward N. Janoff. "Influenza in immunosuppressed populations: a review of infection frequency, morbidity, mortality, and vaccine responses." *The Lancet infectious diseases* 9.8 (2009): 493-504.
5. Lopez, Anthony, et al. "Vaccination recommendations for the adult immunosuppressed patient: A systematic review and comprehensive field synopsis." *Journal of Autoimmunity* 80 (2017): 10-27.
6. Parker, Siddhartha, et al. "A quality improvement project significantly increased the vaccination rate for immunosuppressed patients with IBD." *Inflammatory Bowel Diseases* 19.9 (2013): 1809-1814.
7. Rotondo, John Charles, et al. "SARS-CoV-2 infection: new molecular, phylogenetic, and pathogenetic insights. Efficacy of current vaccines and the potential risk of variants." *Viruses* 13.9 (2021): 1687.
8. Nunes, Danilo Rosa, et al. "Deep phylogenetic-based clustering analysis uncovers new and shared mutations in SARS-CoV-2 variants as a result of directional and convergent evolution." *PloS one* 17.5 (2022): e0268389.

9. Junejo, Yasmeen, et al. "Novel SARS-CoV-2/COVID-19: origin, pathogenesis, genes and genetic variations, immune responses and phylogenetic analysis." *Gene reports* 20 (2020): 100752.
10. Wrapp, Daniel, et al. "Cryo-EM structure of the 2019-nCoV spike in the prefusion conformation." *Science* 367.6483 (2020): 1260-1263.
11. Shang, Jian, et al. "Structural basis of receptor recognition by SARS-CoV-2." *Nature* 581.7807 (2020): 221-224.
12. Bahremand, Taraneh, et al. "COVID-19 hospitalisations in immunocompromised individuals in the Omicron era: a population-based observational study using surveillance data in British Columbia, Canada." *The Lancet Regional Health–Americas* 20 (2023).
13. Wilk, Aaron J., et al. "A single-cell atlas of the peripheral immune response in patients with severe COVID-19." *Nature medicine* 26.7 (2020): 1070-1076.
14. Mueller, Scott N., and Barry T. Rouse. "Immune responses to viruses." *Clinical Immunology* (2008): 421.
15. Weiner, George J. "Rituximab: mechanism of action." *Seminars in hematology*. Vol. 47. No. 2. WB Saunders, 2010.
16. Allison, Anthony C., and Elsie M. Eugui. "Mycophenolate mofetil and its mechanisms of action." *Immunopharmacology* 47.2-3 (2000): 85-118.
17. Maltzman, Jonathan S., and Gary A. Koretzky. "Azathioprine: old drug, new actions." *The Journal of clinical investigation* 111.8 (2003): 1122-1124.

18. Tian, Henghe, and Bruce N. Cronstein. "Understanding the mechanisms of action of methotrexate." *Bull NYU Hosp Jt Dis* 65.3 (2007): 168-173.
19. Fox, Robert I. "Mechanism of action of hydroxychloroquine as an antirheumatic drug." *Seminars in arthritis and rheumatism.* Vol. 23. No. 2. WB Saunders, 1993.
20. Pickup, M. E. "Clinical pharmacokinetics of prednisone and prednisolone." *Clinical pharmacokinetics 4* (1979): 111-128.
21. Comarmond, Cloé, and Patrice Cacoub. "Granulomatosis with polyangiitis (Wegener): clinical aspects and treatment." *Autoimmunity reviews* 13.11 (2014): 1121-1125.
22. Guillevin, Loïc, et al. "Microscopic polyangiitis: clinical and laboratory findings in eighty-five patients." *Arthritis & Rheumatism: Official Journal of the American College of Rheumatology* 42.3 (1999): 421-430.
23. Gioffredi, Andrea, et al. "Eosinophilic granulomatosis with polyangiitis: an overview." *Frontiers in immunology* 5 (2014): 549.
24. Mok, C. C., and C. S. Lau. "Pathogenesis of systemic lupus erythematosus." *Journal of clinical pathology* 56.7 (2003): 481-490.
25. Bannatyne, GilbertA, and ArthurS Wohlmann. "Rheumatoid arthritis: its clinical history, etiology, and pathology." *The Lancet* 147.3791 (1896): 1120-1125.
26. Brito-Zerón, Pilar, et al. "Sjögren syndrome." *Nature reviews Disease primers* 2.1 (2016): 1-20.
27. Almaani, Salem, Alexa Meara, and Brad H. Rovin. "Update on lupus nephritis." *Clinical journal of the American Society of Nephrology: CJASN* 12.5 (2017): 825.

28. Donadio, James V., and Joseph P. Grande. "IgA nephropathy." *New England Journal of Medicine* 347.10 (2002): 738-748.
29. Glassock, Richard J. "Diagnosis and natural course of membranous nephropathy." *Seminars in nephrology*. Vol. 23. No. 4. WB Saunders, 2003.
30. D'Agati, Vivette D., Frederick J. Kaskel, and Ronald J. Falk. "Focal segmental glomerulosclerosis." *New England Journal of Medicine* 365.25 (2011): 2398-2411.
31. Waldman, Meryl, et al. "Adult minimal-change disease: clinical characteristics, treatment, and outcomes." *Clinical Journal of the American Society of Nephrology* 2.3 (2007): 445-453.
32. Plotkin, Stanley A. "Correlates of protection induced by vaccination." *Clinical and vaccine immunology* 17.7 (2010): 1055-1065.
33. Berger, Abi. "Th1 and Th2 responses: what are they?." *Bmj* 321.7258 (2000): 424.
34. Fouser, Lynette A., et al. "Th17 cytokines and their emerging roles in inflammation and autoimmunity." *Immunological reviews* 226.1 (2008): 87-102.
35. Olatunde, Adesola C., J. Scott Hale, and Tracey J. Lamb. "Cytokine-skewed Tfh cells: functional consequences for B cell help." *Trends in immunology* 42.6 (2021): 536-550.
36. Dong, Chen. "Cytokine regulation and function in T cells." *Annual review of immunology* 39 (2021): 51-76.
37. Liu, Chao, et al. "Cytokines: from clinical significance to quantification." *Advanced Science* 8.15 (2021): 2004433.

38. Shahidi, Neal, et al. "Performance of interferon-gamma release assays in patients with inflammatory bowel disease: a systematic review and meta-analysis." *Inflammatory bowel diseases* 18.11 (2012): 2034-2042.
39. Grant, Charlotte R., et al. "Immunosuppressive drugs affect interferon (IFN)-γ and programmed cell death 1 (PD-1) kinetics in patients with newly diagnosed autoimmune hepatitis." *Clinical & Experimental Immunology* 189.1 (2017): 71-82.
40. Sloand, Elaine, et al. "Intracellular interferon-γ in circulating and marrow T cells detected by flow cytometry and the response to immunosuppressive therapy in patients with aplastic anemia." *Blood, The Journal of the American Society of Hematology* 100.4 (2002): 1185-1191.
41. Sauls, Ryan S., Cassidy McCausland, and Bryce N. Taylor. "Histology, T-Cell Lymphocyte." (2018).
42. Golubovskaya, Vita, and Lijun Wu. "Different subsets of T cells, memory, effector functions, and CAR-T immunotherapy." *Cancers* 8.3 (2016): 36.
43. Ruiz-Argüelles, Alejandro. "T lymphocytes in autoimmunity." *Autoimmunity: From Bench to Bedside [Internet]*. El Rosario University Press, 2013.
44. Marani, Marco, et al. "Intensity and frequency of extreme novel epidemics." *Proceedings of the National Academy of Sciences* 118.35 (2021): e2105482118.
45. Zhu, Yajuan, Shuang Liu, and Dingmei Zhang. "Effectiveness of COVID-19 vaccine booster shot compared with non-booster: A meta-analysis." *Vaccines* 10.9 (2022): 1396.